14th World Congress on Computational Mechanics (WCCM)
ECCOMAS Congress 2020
Virtual Congress: 11-15 January 2021
F. Chinesta, R. Abgrall, O. Allix and M. Kaliske (Eds)

AN ADJOINT METHOD FOR THE OPTIMAL BOUNDARY CONTROL OF TURBULENT FLOWS MODELED WITH THE RANS SYSTEM

Andrea Chierici[1], Leonardo Chirco[1], Valentina Giovacchini[1] and Sandro Manservisi[1]

[1] Department of Industrial Engineering DIN
Laboratory of Montecuccolino
University of Bologna
Via dei Colli 16, Bologna, 40136 (BO), Italy

Email: valentin.giovacchin2@unibo.it

Key words: Optimal control theory, adjoint method, boundary control, turbulence, RANS system.

Abstract. In recent years, the optimal control in fluid dynamics has gained attention for the design and the optimization of engineering devices. One of the main challenges concerns the application of the optimal control theory to turbulent flows modeled by the Reynolds averaging Navier-Stokes equations. In this work we propose the implementation of an optimal boundary control problem for the Reynolds-Averaged Navier-Stokes system closed with a two-equations turbulence model. The optimal boundary velocity is sought in order to achieve several objectives such as the enhancement of turbulence or the matching of the velocity field over a well defined domain region. The boundary where the control acts can be the main inlet section or additional injection holes placed along the domain. By minimizing the augmented Lagrangian functional we obtain the optimality system comprising the state, the adjoint, and the control equations. Furthermore, we propose numerical strategies that allow to solve the optimality system in a robust way for such a large number of unknowns.

1 INTRODUCTION

In last years a considerable progress has been made in mathematical analysis and optimal control problems in several research fields of fluid dynamics. Optimal control theory has been applied successfully to many fields ranging from heat transfer problems to fluid-structure interaction systems. Most of the works refer to the standard Navier-Stokes system [1, 2], and the problem of turbulence is usually not taken into account because of the many difficulties arising from the numerical implementation and solution of the optimality system. Optimal control theory applied to DNS simulations for turbulent flows need a very high computational effort and it can be affordable only for simple and two-dimensional geometries [3]. To overcome this issue, in this work we consider the Reynolds averaged Navier-Stokes (RANS) system for the computation of the averaged fields. The closure of the problem is guaranteed by the implementation of a k-ω model for the estimation of eddy viscosity ν_t.

Distributed control strategies and feedback controls have been successfully achieved in previous works both for Navier-Stokes and RANS system [4, 5, 6]. On the other hand, few attempts of optimal boundary control for turbulent flows have been studied. In [7] the turbulence is controlled acting on the wall temperature and the buoyancy forces. In [8] a lifting function approach has been implemented in order to reformulate a boundary control problem into a distributed one for the RANS system closed with the Wilcox k-ω model. According to this approach, boundary controls are defined in the appropriate function boundary spaces restriction of the natural state volume spaces. However, the lifting function is solved in an extension of the domain leading to a higher computational effort. We propose instead a traditional approach for the optimal boundary control and we aim to find the optimal velocity field in the inlet sections of channels in order to achieve some objectives.

In this work we treat optimal control problems for the stationary Reynolds averaged Navier-Stokes equations closed with a k-ω model. We consider an adjoint boundary control problem for steady incompressible turbulent flows, in order to find the optimal boundary velocity that minimizes a functional computed for different objectives. In the first case, we aim at matching the velocity field in a region of the domain with desired values. In the second case, we seek to enhance the turbulence inside the channel. In both cases, goals are accomplished by the injection of fluid with a certain velocity from injection sections. We first derive, by applying the Lagrange multipliers method, the optimality system which consists of the state, adjoint and control equations and then present numerical results by using a steepest descent algorithm for the search of the local minimum of the functional.

2 MATHEMATICAL MODEL

In this section we first report the conservation equations modeling the physical system, then, define the optimal control problem and finally, through the Lagrange multipliers method, achieve the optimality system. We use the standard notation for Lebesgue and Sobolev space. Let $L^2(\Omega)$ denote the space of square-integrable functions in the domain Ω and let $H^s(\Omega)$ indicate the standard Sobolev space with norm $||\cdot||_s$. We denote with $H^{\frac{1}{2}}(\Gamma)$ the trace space for the functions in $H^1(\Omega)$ and its dual space with $H^{-\frac{1}{2}}(\Gamma)$.

2.1 Governing equations

We consider the Reynolds-Averaged Navier-Stokes system for incompressible flows where the Reynolds stress tensor is modeled according to the Boussinesq assumption by using mean velocity gradient components and the eddy viscosity ν_t. We use the Wilcox k-ω model to close the system and accurately evaluate ν_t [9]. The governing equations for turbulent flows in a domain Ω can be written as follows

$$\nabla \cdot \mathbf{u} = 0\,, \tag{1}$$

$$\mathbf{u} \cdot \nabla \mathbf{u} - \nabla \cdot [(\nu + \nu_t)\mathbf{S}(\mathbf{u})] + \nabla p = 0\,, \tag{2}$$

$$\mathbf{u} \cdot \nabla k - \nabla \cdot [(\nu + \sigma_k \nu_t)\nabla k] = P_k - \beta_k k \omega\,, \tag{3}$$

$$\mathbf{u} \cdot \nabla \omega - \nabla \cdot [(\nu + \sigma_\omega \nu_t)\nabla \omega] = c_\omega \frac{\omega}{k} P_k - \beta_\omega \omega^2 + \frac{\sigma_d}{\omega} \nabla k \cdot \nabla \omega\,. \tag{4}$$

The quantity ν_t is the turbulent or eddy viscosity defined in the turbulence model as

$$\nu_t = \min\left(\frac{k}{\omega}, \nu_{t,max}\right)\,. \tag{5}$$

For the interested reader the closure coefficients appearing in (3)-(5) are discussed in details in [10]. The turbulent kinetic energy source term P_k is defined by

$$P_k = \frac{\nu_t}{2}\mathbf{S}(\mathbf{u})^2\,, \tag{6}$$

with $\mathbf{S}(\mathbf{u})^2 = \mathbf{S}(\mathbf{u}) : \mathbf{S}(\mathbf{u})$, where $\mathbf{S}(\mathbf{u})$ is the deformation tensor

$$\mathbf{S}(\mathbf{u}) = \nabla\mathbf{u} + \nabla\mathbf{u}^T\,. \tag{7}$$

We use a near-wall approach for the boundary conditions of the turbulence problem. We set the boundary conditions along the linear region at a distance y_d from the wall, so that the value of ω remains limited in the computational domain

$$\mathbf{u}\cdot\hat{\mathbf{n}} = 0, \quad \mathbf{S}(\mathbf{u})\cdot\hat{\mathbf{n}} = \frac{\mathbf{u}\cdot\hat{\mathbf{t}}}{y_d}, \quad \nabla k\cdot\hat{\mathbf{n}} = \frac{2k}{y_d}, \quad \omega = \frac{2\nu}{\beta_k y_d^2} \quad \text{on } \Gamma_w\,. \tag{8}$$

2.2 Boundary control and cost functional

The first step to obtain the optimality system is to choose an objective for our optimal control problem. The objective functional is denoted by $\mathcal{F}(\mathbf{u},k)$ and is described by the following expression

$$\mathcal{F}(\mathbf{u},k) = \frac{a}{2}\int_{\Omega_d} ||\mathbf{u}-\mathbf{u}_d||^2 d\Omega + \frac{b}{2}\int_{\Omega_d} ||k-k_d||^2 d\Omega\,, \tag{9}$$

where a and b are weight functions. If $a \neq 0$ and $b = 0$ we have a velocity matching problem and objective is expressed by the L^2-norm distance between the velocity field and the desired value $\mathbf{u}_d$. If $b \neq 0$ and $a = 0$ the objective concerns the turbulent kinetic energy and its distance from the target value k_d.

Let Γ_c be a subset of the boundary Γ of the domain $\Omega \subset \mathbb{R}^3$. We introduce the boundary condition

$$\mathbf{u} = \mathbf{u}_c \quad \text{on } \Gamma_c\,, \tag{10}$$

where $\mathbf{u}_c \in H^{\frac{1}{2}}(\Gamma_c)$ is the trace restriction of velocity field $\mathbf{u} \in H^1(\Omega)$. The function $\mathbf{u}_c$ is the control parameter that we aim to optimize in order to achieve some objectives.

In standard boundary control approaches the objective or cost functional is reformulated as

$$\mathcal{J}(\mathbf{u},k,\mathbf{u}_c) = \mathcal{F}(\mathbf{u},k) + \frac{\lambda_1}{2}\int_{\Gamma_c} ||\mathbf{u}_c||^2 d\Gamma + \frac{\lambda_2}{2}\int_{\Gamma_c} ||\nabla_s\mathbf{u}_c||^2 d\Gamma, \tag{11}$$

where ∇_s represents the surface gradient operator. The last two terms are penalization contributions introduced to limit the size of control parameter $\mathbf{u}_c$ and its gradient $\nabla_s\mathbf{u}_c$. In this way, the boundary control parameter is limited to Sobolev space $H^1(\Gamma_c)$, although its natural space is $H^{\frac{1}{2}}(\Gamma_c)$. To enforce $\mathbf{u}_c$ to belong to its natural space it is possible to implement a fractional norm or to adopt a lifting function approach already presented in [8]. In this work we choose to enforce stronger regularity requirements.

The values of λ_1 and λ_2 are important for the solution of the optimal control problem. If $\lambda_2 = 0$, the control variable $\mathbf{u}_c$ belongs to $L^2(\Gamma_c)$, i.e. in a less regular space than its natural one. In the same way, if $\lambda_1 \to 0$, the control variable tends to belong to distributional spaces. For this reason low values of penalization coefficients may lead to convergence issues in the numerical solution of the optimality system. On the other hand, high values of λ_1 and λ_2 may result in too smooth control and poor optimization [11].

2.3 Optimality system

In order to obtain the adjoint equations and the optimality system, the augmented Lagrangian functional is written considering the cost functional $\mathcal{J}(\mathbf{u},k,\mathbf{u}_c)$ and the constraints expressed in the system (1-5) multiplied by appropriate Lagrange multipliers. To reproduce the inequality constraint in (5), we introduce auxiliary variables and transform the inequality into an equality constraint that can be treated with standard techniques. We write condition (5) as

$$\Big(\nu_t - \frac{k}{\omega}\Big)\Big(\nu_t - \nu_{t,max}\Big) = 0\,, \tag{12}$$

and we introduce two new real variables γ_1 and γ_2 defined by

$$\gamma_1^2 = \nu_{t,max} - \nu_t\,, \tag{13}$$

$$\gamma_2^2 = \frac{k}{\omega} - \nu_t\,. \tag{14}$$

The condition (12) is satisfied if $\nu_t = k/\omega$ or $\nu_t = \nu_{t,max}$. If $k/\omega > g$, ν_t must be equal to $\nu_{t,max}$ in order to verify (13) and (14), since left hand side terms are always positive. We also introduce the Lagrange multiplier τ_a to enforce the boundary condition (10). The augmented Lagrangian functional is given by the following expression

$$\begin{aligned}
&\mathcal{L}(\mathbf{u},p,k,\omega,\nu_t,\gamma_1,\gamma_2,\mathbf{u}_c,\mathbf{u}_a,p_a,k_a,\omega_a,\nu_a,\gamma_{a1},\gamma_{a2},\tau_a) = \mathcal{J}(\mathbf{u},k,\mathbf{u}_c) + \int_\Omega p_a \nabla\cdot\mathbf{u}\, d\Omega \\
&+ \int_\Omega \mathbf{u}_a \cdot \Big\{\mathbf{u}\cdot\nabla\mathbf{u} + \nabla p - \nabla\cdot[(\nu+\nu_t)\mathbf{S}(\mathbf{u})]\Big\} d\Omega + \int_{\Gamma_c} \tau_a\cdot(\mathbf{u}-\mathbf{u}_c)\, d\Gamma \\
&+ \int_\Omega k_a \Big\{\mathbf{u}\cdot\nabla k - \nabla\cdot[(\nu+\sigma_k\nu_t)\nabla k] - \frac{\nu_t}{2}\mathbf{S}(\mathbf{u}):\mathbf{S}(\mathbf{u}) + \beta_k k\omega\Big\} d\Omega \\
&+ \int_\Omega \omega_a \Big\{\mathbf{u}\cdot\nabla\omega - \nabla\cdot[(\nu+\sigma_\omega\nu_t)\nabla\omega] - \frac{c_\omega}{2}\mathbf{S}(\mathbf{u}):\mathbf{S}(\mathbf{u}) + \beta_\omega\omega^2 + \frac{\sigma_d}{\omega}\nabla k\cdot\nabla\omega\Big\} d\Omega \\
&+ \int_\Omega \nu_a\Big(\nu_t - \frac{k}{\omega}\Big)(\nu_t - \nu_{t,max})\, d\Omega + \int_\Omega \gamma_{a1}(\gamma_1^2 - \nu_{t,max} + \nu_t)\, d\Omega + \int_\Omega \gamma_{a2}\Big(\gamma_2^2 - \frac{k}{\omega} + \nu_t\Big) d\Omega\,,
\end{aligned} \tag{15}$$

We use label a to denote the Lagrange multipliers $(\mathbf{u}_a,p_a,k_a,\omega_a,\nu_a,\gamma_{a1},\gamma_{a2})$ of the corresponding state variables $(\mathbf{u},p,k,\omega,\nu_t,\gamma_1,\gamma_2)$.

To obtain the optimality system we impose the first order necessary condition $\delta\mathcal{L} = 0$ [11]. In the following we denote with δq the variation of a generic function q and with $(D\mathcal{L}/Dq)\delta q$ the Fréchet derivative of the functional $\mathcal{L}$ in the direction δq. The stationary points of the Lagrangian functional can be found by setting to zero the Fréchet derivatives taken with respect to all the variables, since each variation is independent from the others. When the derivatives are taken with respect to the adjoint variables $(\mathbf{u}_a,p_a,k_a,\omega_a,\nu_a,\gamma_{a1},\gamma_{a2},\tau_a)$, the state system is recovered together with the boundary conditions. To obtain the weak form of the adjoint or dual system, we take the Fréchet derivatives with respect to the state variables $(\mathbf{u},p,k,\omega,\nu_t,\gamma_1,\gamma_2)$.

Considering the variations δp and $\delta\mathbf{u}$, we obtain

$$\int_\Omega \nabla\cdot\mathbf{u}_a\delta p\, d\Omega - \int_\Gamma \mathbf{u}_a\cdot\hat{\mathbf{n}}\delta p\, d\Gamma = 0\,, \qquad \forall\delta p\in L^2(\Omega) \tag{16}$$

$$
\begin{aligned}
&\int_\Omega \{(\delta\mathbf{u}\cdot\nabla)\mathbf{u}\cdot\mathbf{u}_a-(\mathbf{u}\cdot\nabla)\mathbf{u}_a\cdot\delta\mathbf{u}-\nabla p_a\cdot\delta\mathbf{u}-\nabla\cdot[(\nu+\nu_t)\mathbf{S}(\mathbf{u}_a)]\cdot\delta\mathbf{u}\\
&\quad+k_a\nabla k\cdot\delta\mathbf{u}+\omega_a\nabla\omega\cdot\delta\mathbf{u}+\nabla\cdot[(k_a\nu_t+c_\omega\omega_a)\mathbf{S}(\mathbf{u})]\cdot\delta\mathbf{u}\}d\Omega=\\
&\quad=\int_\Gamma\{-p_a\hat{\mathbf{n}}\cdot\delta\mathbf{u}-(\mathbf{u}\cdot\hat{\mathbf{n}})(\mathbf{u}_a\cdot\delta\mathbf{u})+(\nu+\nu_t)\mathbf{S}(\delta\mathbf{u})\cdot\hat{\mathbf{n}}\cdot\mathbf{u}_a \qquad \forall\delta\mathbf{u}\in\mathbf{H}^1(\Omega)\\
&\quad+(k_a\nu_t+c_\omega\omega_a)\mathbf{S}(\mathbf{u})\cdot\delta\mathbf{u}\cdot\hat{\mathbf{n}}-(\nu+\nu_t)\mathbf{S}(\mathbf{u}_a)\cdot\delta\mathbf{u}\cdot\hat{\mathbf{n}}\}d\Gamma\\
&\quad-\int_{\Gamma_c}\tau_a\cdot\delta\mathbf{u}d\Gamma
\end{aligned}
\tag{17}
$$

The natural boundary conditions for the optimality system in strong form can be obtained setting equal to zero the surface integrals containing unknown terms or non-integrable functions. Let be Γ_c the controlled surface, Γ_w the walls, Γ_o the outlet and $\Gamma_c\cup\Gamma_w\cup\Gamma_o=\Gamma$.

Over Γ_c, we set $\mathbf{u}_a=0$, $k_a=\omega_a=0$ and $p_a=0$, then we can deduce the expression of the Lagrangian multiplier $\tau_a\in H^{-1}(\Gamma_c)$

$$
\tau_a=-(\nu+\nu_t)\mathbf{S}(\mathbf{u}_a)\cdot\hat{\mathbf{n}}\quad \text{on } \Gamma_c\,. \tag{18}
$$

In the outlet section Γ_o, we have for the state variables $\mathbf{S}(\mathbf{u})\cdot\hat{\mathbf{n}}=0$ and $p=0$. In order to enforce the integration to vanish, we have

$$
p_a=0,\quad (\nu+\nu_t)\mathbf{S}(\mathbf{u}_a)\cdot\hat{\mathbf{n}}=(\mathbf{u}\cdot\hat{\mathbf{n}})\mathbf{u}_a\quad \text{on } \Gamma_o\,. \tag{19}
$$

The conditions for the state variables over Γ_w are reported in (8) and therefore the boundary integral vanishes with

$$
\mathbf{u}_a\cdot\hat{\mathbf{n}}=0,\quad \omega_a=0,\quad (\nu+\nu_t)\mathbf{S}(\mathbf{u}_a)\cdot\hat{\mathbf{n}}=\frac{k_a\nu_t\mathbf{u}\cdot\hat{\mathbf{t}}}{y_d}\quad \text{on } \Gamma_w\,. \tag{20}
$$

The conditions so defined are appropriate also to vanish the boundary integral in (16). We now consider the variations of the total Lagrange functional in the directions δk and $\delta\omega$. The Fréchet derivatives in the directions δk and $\delta\omega$ are independent and should be zero in order to minimize the functional. We integrate by parts and extract each variation from the differential operators

$$
\begin{aligned}
&\int_\Omega\Big\{-(\mathbf{u}\cdot\nabla)k_a-\nabla\cdot\Big[\Big(\nu+\sigma_k\nu_t\Big)\nabla k_a\Big]+\beta_k\omega k_a+b(k-k_d)-\frac{\nu_a(\nu_t-\nu_{t,max})+\gamma_{a2}}{\omega}\\
&\quad-\sigma_d\nabla\cdot\Big[\frac{\omega_a}{\omega}\nabla\omega\Big]\Big\}\delta k d\Omega+\int_\Gamma\Big[\mathbf{u}\cdot\hat{\mathbf{n}}k_a\delta k-(\nu+\sigma_k\nu_t)\nabla\delta k\cdot\hat{\mathbf{n}}k_a\\
&\quad+\frac{\omega_a}{\omega}\sigma_d\nabla\omega\cdot\hat{\mathbf{n}}\delta k+(\nu+\sigma_k\nu_t)\nabla k_a\cdot\hat{\mathbf{n}}\delta k\Big]d\Gamma=0\,,\qquad \forall\delta k\in H^1(\Omega)\,,
\end{aligned}
\tag{21}
$$

$$
\begin{aligned}
&\int_\Omega\Big\{-(\mathbf{u}\cdot\nabla)\omega_a-\nabla\cdot\Big[\Big(\nu+\sigma_\omega\nu_t\Big)\nabla\omega_a\Big]+2\beta_\omega\omega\omega_a+\frac{k\gamma_{a2}+k\nu_a(\nu_t-\nu_{t,max})}{\omega^2}+\beta_k k k_a\\
&\quad-\sigma_d\frac{\omega_a\nabla k\cdot\nabla\omega}{\omega^2}-\sigma_d\nabla\cdot\Big(\frac{\omega_a}{\omega}\nabla k\Big)\Big\}\delta\omega d\Omega+\int_\Gamma\Big[\mathbf{u}\cdot\hat{\mathbf{n}}\omega_a\delta\omega-(\nu+\sigma_\omega\nu_t)\nabla\delta\omega\cdot\hat{\mathbf{n}}\omega_a\\
&\quad+\sigma_d\frac{\omega_a}{\omega}\nabla k\cdot\hat{\mathbf{n}}\delta\omega+(\nu+\sigma_\omega\nu_t)\nabla\omega_a\cdot\hat{\mathbf{n}}\delta\omega\Big]d\Gamma=0\,,\qquad \forall\delta\omega\in H^1(\Omega)\,.
\end{aligned}
\tag{22}
$$

Setting equal to zero the surface integrals, we obtain the remaining boundary conditions. Over Γ_o, we have for the state variables $\nabla\omega\cdot\hat{\mathbf{n}}=\nabla k\cdot\hat{\mathbf{n}}=0$ which implies

$$
(\nu+\sigma_k\nu_t)\nabla k_a\cdot\hat{\mathbf{n}}=-\mathbf{u}\cdot\hat{\mathbf{n}}k_a,\quad (\nu+\sigma_\omega\nu_t)\nabla\omega_a\cdot\hat{\mathbf{n}}=-\mathbf{u}\cdot\hat{\mathbf{n}}\omega_a, \tag{23}
$$

Over Γ_w, we have used the near wall approach (8) for state variables. For the adjoint variables, we obtain

$$\omega_a = 0, \quad \nabla k_a \cdot \hat{\mathbf{n}} = \frac{2k_a}{y_d}\,. \tag{24}$$

We now consider the variations of the total Lagrange functional in the direction $\delta\nu_t$ and integrate by parts to extract each variation from differential operators

$$\int_\Omega \Big[\mathbf{S}(\mathbf{u}) : \nabla \mathbf{u}_a + \sigma_k \nabla k \cdot \nabla k_a - \frac{k_a}{2}\mathbf{S}(\mathbf{u}) : \mathbf{S}(\mathbf{u}) + \sigma_\omega \nabla\omega \cdot \nabla\omega_a + \nu_a\Big(2\nu_t - \nu_{t,max} - \frac{k}{\omega}\Big) \\ + \gamma_{a1} + \gamma_{a2}\Big]\delta\nu_t d\Omega - \int_\Gamma (\mathbf{S}(\mathbf{u}) \cdot \hat{\mathbf{n}} \cdot \mathbf{u}_a - \sigma_k \nabla k \cdot \hat{\mathbf{n}} - \sigma_\omega \nabla\omega \cdot \hat{\mathbf{n}})\delta\nu_t d\Gamma = 0\,, \qquad \forall \delta\nu_t \in L^2(\Omega)\,. \tag{25}$$

The boundary conditions previously described make the surface integrals equal to zero. If we consider the variations of Lagrange functional with respect to the constraints $\delta\gamma_1$ and $\delta\gamma_2$ we obtain

$$\int_\Omega 2\gamma_1\gamma_{a1}\delta\gamma_1 d\Omega = 0\,, \tag{26}$$

$$\int_\Omega 2\gamma_2\gamma_{a2}\delta\gamma_2 d\Omega = 0\,, \tag{27}$$

that are algebraic equations. If $\nu_t = k/\omega$ then $\gamma_2 = 0$, $\gamma_1 > 0$ and $\gamma_{a1} = 0$. In this case we can set $\gamma_{a1} = \nu_a(1 - \nu_t + k/\omega)$. If $\nu_t = \nu_{t,max}$ then $\gamma_1 = 0$, $\gamma_2 > 0$ and $\gamma_{a1} = 0$ while for γ_{a2} we can set $\gamma_{a2} = \nu_a(1 - \nu_t + \nu_{t,max})$. In this way, in both cases we can solve (25) for ν_a obtaining

$$\nu_a = \frac{k_a}{2}\mathbf{S}(\mathbf{u}) : \mathbf{S}(\mathbf{u}) - \mathbf{S}(\mathbf{u}) : \nabla\mathbf{u}_a - \sigma_k \nabla k \cdot \nabla k_a - \sigma_\omega \nabla\omega \cdot \nabla\omega_a\,. \tag{28}$$

Finally for the variation $\delta\mathbf{u}_c$ of the control $\mathbf{u}_c$ we have

$$\int_{\Gamma_c} (\lambda_1 \mathbf{u}_c \cdot \delta\mathbf{u}_c + \lambda_2 \nabla_s \mathbf{u}_c : \nabla_s \delta\mathbf{u}_c - \tau_a \cdot \delta\mathbf{u}_c) d\Gamma = 0\,, \qquad \forall \delta\mathbf{u}_c \in \mathbf{H}^1(\Gamma_c)\,. \tag{29}$$

By substituting the equation (18) we obtain

$$\int_{\Gamma_c} (\lambda_1 \mathbf{u}_c \cdot \delta\mathbf{u}_c + \lambda_2 \nabla_s \mathbf{u}_c : \nabla_s \delta\mathbf{u}_c + (\nu + \nu_t)\mathbf{S}(\mathbf{u}_a) \cdot \hat{\mathbf{n}} \cdot \delta\mathbf{u}_c) d\Gamma = 0\,. \tag{30}$$

If $\lambda_2 = 0$, equation (30) simplifies in the following algebraic expression

$$\mathbf{u_c} = -\frac{(\nu + \nu_t)}{\lambda_1}\mathbf{S}(\mathbf{u}_a) \cdot \hat{\mathbf{n}} \text{ on } \Gamma_c\,. \tag{31}$$

The boundary control $\mathbf{u}_c$ on the boundary Γ_c depends on the adjoint velocity surface normal gradient $(\nabla\mathbf{u}_a + \nabla\mathbf{u}_a^T) \cdot \hat{\mathbf{n}}$, on eddy viscosity ν_t and on regularization parameters λ_1 and λ_2.

The variations with respect to the adjoint variables give back the original state system (1)-(5). In the case one might be interested in a finite volume discretization it is necessary to recover the strong form of the adjoint system

$$\nabla \cdot \mathbf{u}_a = 0 \tag{32}$$

$$
\begin{aligned}
(\mathbf{u}\cdot\nabla)\mathbf{u}_a-(\nabla\mathbf{u})^T\cdot\mathbf{u}_a=&-\nabla p_a-\nabla\cdot[(\nu+\nu_t)\mathbf{S}(\mathbf{u}_a)]+k_a\nabla k+\omega_a\nabla\omega\\
&+\nabla\cdot[(k_a\nu_t+c_\omega\omega_a)\mathbf{S}(\mathbf{u})]+a(\mathbf{u}-\mathbf{u}_d)
\end{aligned} \tag{33}
$$

$$
\begin{aligned}
(\mathbf{u}\cdot\nabla)k_a+\nabla\cdot\left[\left(\nu+\sigma_k\nu_t\right)\nabla k_a\right]=&\beta_k\omega k_a+\sigma_d\nabla\cdot\left(\frac{\omega_a}{\omega}\nabla\omega\right)\\
&+b(k-k_d)-\frac{\gamma_{a2}-\nu_a(\nu_t-\nu_{t,max})}{\omega}
\end{aligned} \tag{34}
$$

$$
\begin{aligned}
(\mathbf{u}\cdot\nabla)\omega_a\nabla\cdot\left[\left(\nu+\sigma_\omega\nu_t\right)\nabla\omega_a\right]=&2\beta_\omega\omega\omega_a-\sigma_d\frac{\omega_a}{\omega^2}\nabla k\cdot\nabla\omega-\sigma_d\nabla\cdot\left(\frac{\omega_a}{\omega}\nabla k\right)\\
&+\frac{\nu_a k(\nu_t-\nu_{t,max})+\gamma_{a2}k}{\omega^2}+\beta_k k k_a
\end{aligned} \tag{35}
$$

$$
\nu_a=\frac{k_a}{2}\mathbf{S}(\mathbf{u}):\mathbf{S}(\mathbf{u})-\mathbf{S}(\mathbf{u}):\nabla\mathbf{u}_a-\sigma_k\nabla k\cdot\nabla k_a-\sigma_\omega\nabla\omega\cdot\nabla\omega_a\,. \tag{36}
$$

The optimality system consists of the state system (1)-(5), the adjoint system (32)-(36), the optimality condition (30) and it is completed with the appropriate boundary conditions reported in Table 1.

Table 1: Boundary conditions with a near wall approach for the state variables $(\mathbf{u},p,k,\omega)$ and for the adjoint variables $(\mathbf{u}_a,p_a,k_a,\omega_a)$.

Variable	Γ_C	Γ_W	Γ_O
$\mathbf{u}$	$\mathbf{u}\cdot\hat{\mathbf{n}}=\mathbf{u}_C$	$\mathbf{u}_n=0$	$\mathbf{S}(\mathbf{u})\cdot\hat{\mathbf{n}}=0$
	$\mathbf{u}\cdot\hat{\mathbf{t}}=0$	$(\nu+\nu_t)\mathbf{S}(\mathbf{u})\cdot\hat{\mathbf{n}}=\nu\mathbf{u}\cdot\hat{\mathbf{t}}/y_d$	$\mathbf{u}\cdot\hat{\mathbf{t}}=0$
p	$-$	$-$	$p=0$
k	$k=k_{IN}$	$\nabla k\cdot\hat{\mathbf{n}}=\frac{2k}{y_d}$	$\nabla k\cdot\hat{\mathbf{n}}=0$
ω	$\omega=\omega_{IN}$	$\omega=\frac{2\nu}{\beta_k y_d^2}$	$\nabla\omega\cdot\hat{\mathbf{n}}=0$
$\mathbf{u}_a$	$\mathbf{u}_a\cdot\hat{\mathbf{n}}=0$	$\mathbf{u}_a\cdot\hat{\mathbf{n}}=0$	$(\nu+\nu_t)\mathbf{S}(\mathbf{u}_a)\cdot\hat{\mathbf{n}}=(\mathbf{u}\cdot\hat{\mathbf{n}})\mathbf{u}_a$
	$\mathbf{u}_a\cdot\hat{\mathbf{t}}=0$	$(\nu+\nu_t)\mathbf{S}(\mathbf{u}_a)\cdot\hat{\mathbf{n}}=k_a\nu_t\mathbf{u}\cdot\hat{\mathbf{t}}/y_d$	$\mathbf{S}(\mathbf{u}_a)\cdot\hat{\mathbf{t}}=0$
p_a	$-$	$-$	$p_a=0$
k_a	$k_a=0$	$\nabla k_a\cdot\hat{\mathbf{n}}=2k_a/y_d$	$(\nu+\sigma_k\nu_t)\nabla k_a\cdot\hat{\mathbf{n}}=-\mathbf{u}\cdot\hat{\mathbf{n}}k_a$
ω_a	$\omega_a=0$	$\omega_a=0$	$(\nu+\sigma_\omega\nu_t)\nabla\omega_a\cdot\hat{\mathbf{n}}=-\mathbf{u}\cdot\hat{\mathbf{n}}\omega_a$

A velocity matching objective is easier to be achieved since in the adjoint velocity equation (33) the source term $a(\mathbf{u}-\mathbf{u}_d)$ appears and acts directly on $\mathbf{u}_a$, which appears in its turn in the optimality condition (30). For this reason, a velocity matching objective is easier to be achieved. If a turbulent kinetic energy objective is considered, the source term, $b(k-k_d)$, acts on k_a in (34) and through the adjoint $\mathbf{u}_a$ affects the velocity field to obtain an enhancement or reduction of turbulent kinetic energy. In this case the control is much more complex and the optimality system is strongly coupled.

Due to its strong nonlinearity, the optimality system cannot be solved with one-shot techniques. We use the following steepest descent algorithm:

1. Setup

   a) Set an initial value for the control $\mathbf{u}_c^0$ and an initial state $(\mathbf{u}^0, p^0, k^0, \omega^0, \nu_t^0)$ solution of the state system (1)-(5)
   b) Compute the functional $\mathcal{J}^0$ in (11)
   c) Set $\Delta\mathbf{u}_c^0 = 0$, $r^0 = 1$
2. Solve the adjoint system (32)-(36) for the adjoint variables $(\mathbf{u}_a^i, p_a^i, k_a^i, \omega_a^i, \nu_a^i)$
3. Set the control update $\Delta\mathbf{u}_c^i = \mathbf{u}_c$ by solving (30) and compute $\mathbf{u}_c^i = \mathbf{u}_c^{i-1} + r^{i,j}\Delta\mathbf{u}_c^i$
4. Solve (1)-(5) for the state variables $(\mathbf{u}^{i,j}, p^{i,j}, k^{i,j}, \omega^{i,j}, \nu_t^{i,j})$
5. Compute the functional $\mathcal{J}^{i,j}$ in (11)
   a) if $\|\mathcal{J}^{i,j} - \mathcal{J}^{i,j-1}\| / \mathcal{J}^{i,j-1} < toll$ convergence of the optimal control problem is reached
   b) else if $\mathcal{J}^{i,j} > \mathcal{J}^{i,j-1}$ set $r^{i,j+1} = 0.5 r^{i,j}$ and return to step 3.
   c) else if $\mathcal{J}^{i,j} < \mathcal{J}^{i,j-1}$ set $r^{i,j+1} = r^0$ and return to step 2.

3 Numerical Results

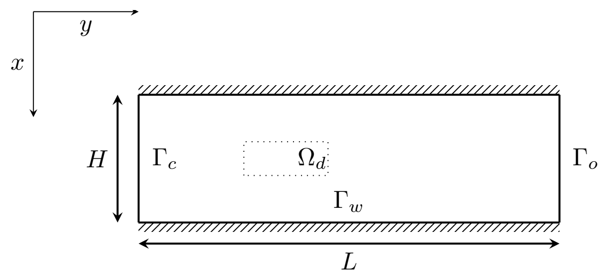

Figure 1: Plane channel geometry.

In this section, we solve the optimality system in a two-dimensional geometry for velocity matching and turbulence enhancement cases. We use a finite element discretization of the optimality system written in weak form, replacing the infinite-dimensional spaces with appropriate finite-dimensional spaces. We use a *differentiate-then-discretize* approach since we apply the finite element approximation after computing the Fréchet differentials. We use quadratic finite elements for all the variables but the pressure, for which we use linear finite elements. The steepest descent algorithm has been implemented in the finite element code FEMuS [12] and the PETSc libraries are used to handle the algebraic solver of the system.

The geometry we have tested is the plane channel with $H = 0.1m$ and $L = 0.0303m$ reported in Figure 1. The rectangular domain Ω is defined as $\Omega = \{(x,y) : x \in [0, 0.0303], y \in [-0.05, 0.05]\}$. The fluid flows from the controlled boundary Γ_c, on the left, to the outflow section Γ_o, on the right, while the region of boundary Γ_w represents the walls where we have set the near-wall boundary conditions as reported in Table 1. The y-axis is set along the flow direction while the x-axis is along the transverse one. The bulk mesh consists of 15655 nodes with mesh refinement near wall boundaries. We have considered liquid lead with density $\rho = 10340 kg/m^3$ and dynamic viscosity $\mu = 0.00181 Pa \cdot s$.

3.1 Test 1. Velocity Matching Case

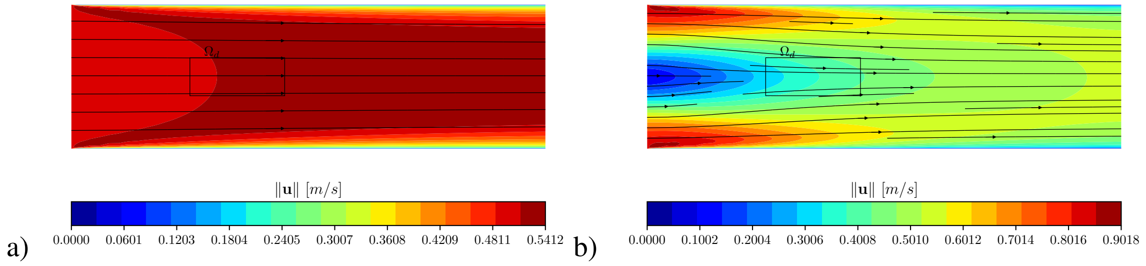

Figure 2: Test 1: Velocity Matching Case. Isosurface contours and streamlines of the velocity for the uncontrolled case (a) and for $\lambda_1 = 10^{-8}$ and $\lambda_2 = 10^{-4}$ (b).

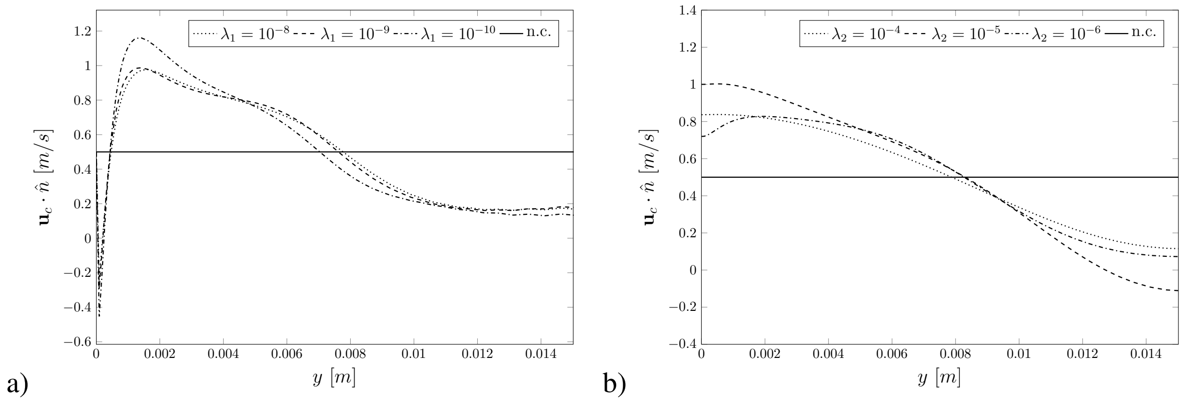

Figure 3: Test 1: Velocity Matching Case. a) Velocity profile over the half-section of Γ_c for tests with $\lambda_1 = 10^{-8}, 10^{-9}, 10^{-10}$ and $\lambda_2 = 0$. b) Velocity profile over the half-section of Γ_c for tests with $\lambda_2 = 10^{-4}, 10^{-5}, 10^{-6}$ and $\lambda_1 = 10^{-9}$.

Let be $\Omega_d = \{(x,y) : x \in [0.01115, 0.01915], y \in [-0.025, -0.005]\}$ the region where we aim to minimize the objective functional with an objective on velocity field, therefore with $a = 1$ and $b = 0$

$$\mathcal{J}(\mathbf{u}, \mathbf{u}_c) = \frac{a}{2} \int_{\Omega_d} ||\mathbf{u} - \mathbf{u}_d||^2 d\Omega + \frac{\lambda_1}{2} \int_{\Gamma_c} ||\mathbf{u}_c||^2 d\Gamma + \frac{\lambda_2}{2} \int_{\Gamma_c} ||\nabla_s \mathbf{u}_c||^2 d\Gamma \,. \tag{37}$$

We have performed several tests varying the regularization parameters $\lambda_1 = 10^{-8}, 10^{-9}, 10^{-10}$ and $\lambda_2 = 10^{-4}, 10^{-5}, 10^{-6}$.

In Figure 2 a) we report the velocity profile over the domain Ω at the reference state. We have set a constant velocity profile $\mathbf{u}_c = (0, 0.5m/s)$ on the boundary Γ_c as initial value for the control, resulting in $Re = uH\rho/\mu = 87000$. Over Ω_d, the velocity field assumes a maximum value of $0.5412m/s$. These simulations aim to control the distance expressed in L^2-norm between the velocity field and a target value. In this test we aim to reduce the velocity over Ω_d with respect to the reference case, therefore we set $\mathbf{u}_d = (0, 0.3m/s)$. In Figure 2 b) the velocity over the domain Ω is reported for the optimal solution corresponding to $\lambda_1 = 10^{-8}$ and $\lambda_2 = 10^{-4}$. Over Ω_d, the velocity assumes values around 0.3-0.4m/s.

Table 2: Test 1: Velocity Matching Case. Objective functionals with $\lambda_2 = 0$ and different λ_1 values. The reference case without control is obtained when $\lambda_1 \to \infty$.

λ_1	∞	10^{-8}	10^{-9}	10^{-10}
$\mathcal{J} \cdot 10^6$	4.26025	1.93769	1.70594	1.00159

Table 3: Test 1: Velocity Matching Case. Objective functional with $\lambda_1 = 10^{-9}$ and different λ_2 values.

λ_2	10^{-4}	10^{-5}	10^{-6}
$\mathcal{J} \cdot 10^6$	4.08514	1.04643	1.00159

To analyze the influence of the regularization parameter λ_1 on the optimal solution, we show in Figure 3 a) the results with $\lambda_2 = 0$ for different values of λ_1. When λ_1 is smaller, the control acts stronger and achieves low values of the objective functional, as the reader can see in Table 2. For the lowest considered value of λ_1, the optimization gives a 77% functional reduction.

In Figure 3 b), we show the influence of the solution on the regularization parameter λ_2. We set $\lambda_1 = 10^{-9}$ and we consider $\lambda_2 = 10^{-4}, 10^{-5}, 10^{-6}$. Figure 3 b) evidences that the highest considered value of λ_2 brings to the smoothest solution and to the poorest functional reduction (around 4%), as reported in Table 3. When low values of λ_2 are considered, the boundary control parameter is closed to the solution obtained with $\lambda_2 = 0$ and brings to the strongest functional reduction.

3.2 Test 2. Turbulence Enhancement Case

Let be $\Omega_d = \{(x,y) : x \in [0.01115, 0.01915], y \in [-0.025, -0.005]\}$ the region where we aim to minimize the objective functional with an objective on turbulent kinetic energy, therefore with $a = 0$ and $b = 1$ in (11)

$$\mathcal{J}(k, \mathbf{u}_c) = \frac{b}{2} \int_{\Omega_d} |k - k_d|^2 d\Omega + \frac{\lambda_1}{2} \int_{\Gamma_c} ||\mathbf{u}_c||^2 d\Gamma + \frac{\lambda_2}{2} \int_{\Gamma_c} ||\nabla_s \mathbf{u}_c||^2 d\Gamma \tag{38}$$

In Figure 4 a) we report the turbulent kinetic energy profile over the domain Ω at the reference state. Also in this case, we have set a constant velocity profile $\mathbf{u}_c = (0, 0.5m/s)$ on the boundary Γ_c as initial value for the control. Over Ω_d, the turbulent kinetic energy assumes values in the order of magnitude about $10^{-4} m^2/s^2$. In order to enhance the turbulence inside the channel, we aim to minimize the distance expressed in L^2-norm between the turbulent kinetic energy and a target value, i.e. $k_d = 0.01 m^2/s^2$. In Figure 4 b) the turbulent kinetic energy over the domain Ω is reported for the optimal solution corresponding to $\lambda_1 = 10^{-13}$ and $\lambda_2 = 10^{-6}$. Over Ω_d, the turbulent kinetic energy assumes values around

Table 4: Test 2: Turbulence enhancement case. Objective functionals with $\lambda_1 = 10^{-13}$ and different λ_2 values.

λ_2	∞	$5 \cdot 10^{-5}$	10^{-5}	$5 \cdot 10^{-6}$
$\mathcal{J} \cdot 10^{10}$	82.7304	19.1531	12.2519	4.55217

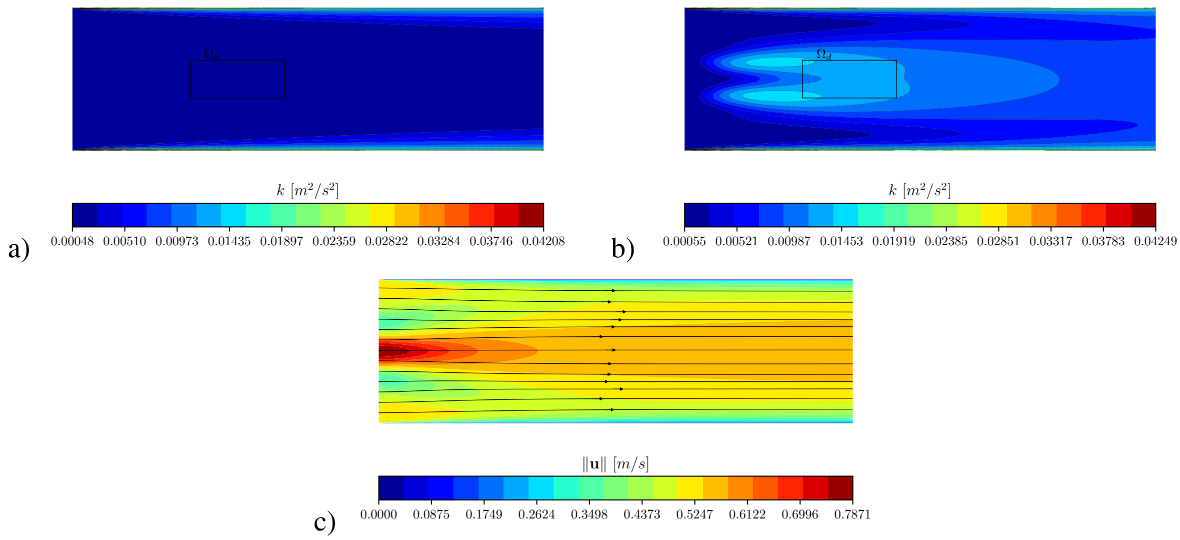

Figure 4: Test 2: Turbulence enhancement case. Isosurface contours of turbulent kinetic energy field for the uncontrolled case (a) and for $\lambda_1 = 10^{-13}$ and $\lambda_2 = 10^{-6}$ (b). Isosurface contours and streamlines of the velocity field corresponding to the optimal state (c).

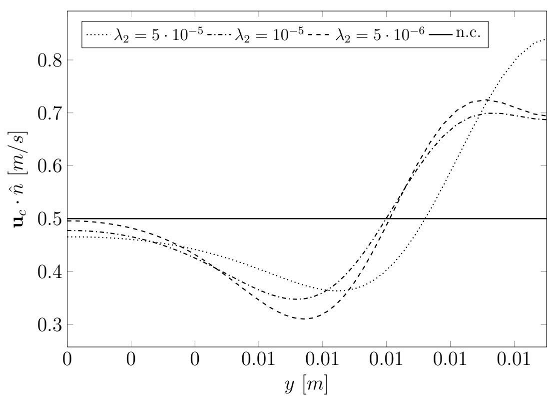

Figure 5: Test 2: Turbulence Enhancement Case. Velocity profiles along the half-section of Γ_c with $\lambda_2 = 5\cdot 10^{-5}, 10^{-5}, 5\cdot 10^{-6}$ and $\lambda_1 = 10^{-13}$.

0.009-0.014m^2/s^2. The corresponding velocity profile over the domain Ω is reported in Figure 4 c). The optimization algorithm leads, with this set of regularization parameters, to a velocity profile with a strong peak in the middle of the channel to maximize the turbulence over Ω_d.

Also in this test case, we show the influence of the solution on the regularization parameter λ_2 in Figure 5. We set $\lambda_1 = 10^{-13}$ and we consider $\lambda_2 = 5\cdot 10^{-5}, 10^{-5}, 5\cdot 10^{-6}$. Figure 5 evidences that the highest considered value of λ_2 brings to the smoothest solution and to the poorest functional reduction (around 77%), as reported in Table 4, while the lowest value of λ_2 brings to the strongest functional reduction (95%).

4 Conclusions

An adjoint-based boundary optimal control method for the Reynolds Averaged Navier-Stokes equations coupled with a two-equations turbulence model has been presented. The adjoint system has been obtained through a Lagrangian functional minimization. Proper boundary conditions have been set on the adjoint variables and a steepest descent algorithm has been implemented for the segregate solution of the optimality system. Simple test cases have been reported to show the robustness of the mathematical approach presented for different objectives and different regularization terms.

REFERENCES

[1] Gunzburger M D, Hou L and Svobodny T P 1992 *SIAM journal on control and optimization* **30** 167–181

[2] Ghattas O and Bark J H 1997 *Journal of Computational Physics* **136** 231–244

[3] Bewley T R, Moin P and Temam R 2001 *Journal of Fluid Mechanics* **447** 179–225

[4] Manservisi S and Menghini F 2016 *Computers & Fluids* **125** 130–143

[5] Manservisi S and Menghini F 2016 *Computers & Mathematics with Applications* **71** 2389–2406

[6] Gunzburger M and Manservisi S 2000 *Comput Methods Appl Mech Eng* **189**(3) 803–823

[7] Chirco L, Giovacchini V and Manservisi S 2020 An adjoint-based temperature boundary optimal control approach for turbulent buoyancy-driven flows *Journal of Physics: Conference Series* vol 1599 (IOP Publishing) p 012041

[8] Chirco L, Chierici A, Da Vià R, Giovacchini V and Manservisi S 2019 Optimal control of the wilcox turbulence model with lifting functions for flow injection and boundary control *Journal of Physics: Conference Series* vol 1224 (IOP Publishing) p 012006

[9] Wilcox D 1994 *Turbulence Modeling for CFD* (DCW Industries, Incorporated)

[10] Wilcox D C 2008 *AIAA journal* **46** 2823–2838

[11] Gunzburger M D 2003 *Perspectives in flow control and optimization* vol 5 (Siam)

[12] FEMuS. URL https://github.com/FemusPlatform/femus